Intermetallics 19 (2011) 321–326

Contents lists available at ScienceDirect

Intermetallics

journal homepage: www.elsevier.com/locate/intermet

Magnetic ordering of novel La_3NiGe_2-type R_3CoGe_2 compounds (R = Pr, Nd, Sm, Gd–Dy)

P. Manfrinetti [a,b], A.V. Morozkin [c,*], O. Isnard [d,e], F. Wrubl [a], Yu. Mozharivskyj [f], V. Svitlyk [f]

[a] Dipartimento di Chimica, Universita` di Genova, Via Dodecaneso 31, 16146 Genova, Italy
[b] CNR-SPIN, Corso Perrone 24, 16152 Genova, Italy
[c] Department of Chemistry, Moscow State University, Leninskie Gory, House 1, Building 3, Moscow, GSP-2, 119992, Russia
[d] Institut Laue-Langevin, 6 Rue J. Horowitz, 38042 Grenoble, France
[e] Laboratoire de Cristallographie du CNRS, Université J. Fourier, BP166X, 38042 Grenoble, France
[f] Department of Chemistry, McMaster University, 1280 Main Street West, Hamilton, Ontario, Canada L8S 4M1

ARTICLE INFO

Article history:
Received 17 August 2010
Received in revised form
13 October 2010
Accepted 18 October 2010
Available online 11 November 2010

Keywords:
A. Rare-earth intermetallics
B. Magnetic properties
F. Neutron diffraction

ABSTRACT

The novel R_3CoGe_2 compounds adopt the La_3NiGe_2-type structure (space group *Pnma*) with the following cell parameters: a = 1.1706(1), b = 0.42267(5), c = 1.1242(1) nm for Sm_3CoGe_2; a = 1.15845(5), b = 0.41905(2), c = 1.12088(5) nm for Gd_3CoGe_2; a = 1.14942(4), b = 0.41705(2), c = 1.11030(4) nm for Tb_3CoGe_2 and a = 1.1431(2), b = 0.41500(5), c = 1.1040(2) nm for Dy_3CoGe_2. The R_3CoGe_2 compounds undergo a ferrimagnetic type ordering (T_{CN} = 150 K for Gd_3CoGe_2). Neutron diffraction studies show that Pr_3CoGe_2 and Nd_3CoGe_2 have a commensurate ferromagnetic component along the a axis and a commensurate antiferromagnetic component along the c axis (**Pn'ma** magnetic space group): $(M^{F}_{Pr})_a$ = 2.59(9) μ_B, $(M^{AF}_{Pr})_c$ = 1.58(4) μ_B, $|M_{Pr}|$ = 3.03(9) μ_B for Pr_3CoGe^2 and $(M^{F}_{Nd})_a$ = 2.6(1) μ_B, $(M^{AF}_{Nd})_c$ = 1.65(6) μ_B, $|M_{Nd}|$ = 3.1(1) μ_B for Nd_3CoGe_2 at 2 K.

Magnetocaloric effect of Gd_3CoGe_2 in terms of the isotherm entropy change, ΔS_{iso}, was derived from the magnetization measurement, and it reaches the maximum value of $\Delta S_{iso} = -4.9$ J/kg•K in the 139–144 K temperature range.

1. Introduction

The R_3NiGe_2 and R_3NiSi_2 compounds with R = La–Sm, Gd–Er adopt the La_3NiGe_2 (Gd_3NiSi_2)-type structure (space group *Pnma*) [1,2,3]. Recently, three novel Co-containing Ce_3CoGe_2, Pr_3CoGe_2 and Nd_3CoGe_2 compounds with the same structure have been obtained [4]. The La_3NiGe_2 structure is a member of the family of the two-layer orthorhombic structures with the *Pnma* symmetry and a set of special 4(c) sites (x, 1/4, z) derived from the hexagonal Mg structure. The Mg-type rare-earth unit cell in the La_3NiGe_2 structure can be represented as follows: the rare-earth atoms occupy three special positions 4(c) (1/3, 1/4, 0), 4(c) (−1/6, 1/4, −1/6) and 4(c) (1/3, 1/4, 1/3), and the cell parameters are $a_{La_3NiGe_2} = a_{Mg}\cdot(3)^{1/2}$, $b_{La_3NiGe_2} = c_{Mg}$, and $c_{La_3NiGe_2} = 3\cdot a_{Mg}$, space group *Pnma* (No 62). Insertion of the transition metal and *p*-element atoms into the Mg-type rare-earth structure leads to an orthorhombic distortion of this structure and formation of the La_3NiGe_2 structure. Such transformation from the rare-earth structure to that of La_3NiGe_2 results in the change of their magnetic properties: the Ce, Pr and Nd substructures in R_3CoGe_2 exhibit ferromagnetic orderings (in addition to lower-temperature antiferromagnetic ones for the Ce and Nd compounds) [4,5] while only antiferromagnetic transitions are present in elemental Ce, Pr, Nd [6], and the magnetic ordering temperatures of the Gd_3NiSi_2 and Gd_3NiGe_2 [7,8] are lower than that of pure Gd [9] (Table 1).

In the present work, neutron diffraction studies and magnetic measurements on R_3CoGe_2 have been carried out to establish the nature of magnetic interactions in this class of intermetallics.

2. Experimental

The R_3CoGe_2 samples were prepared by arc-melting weighed amounts of rare earths (99.9% wt. purity), Co (99.99% wt. purity) and Ge (99.99% wt. purity). The arc-melted Pr_3CoGe_2 and Nd_3CoGe_2 samples were wrapped in a Ta foil, sealed in a silica tube under vacuum and annealed at 1000 °C for 1 month. The {Sm, Gd–Dy}$_3$CoGe$_2$ samples were annealed at 800 °C for 200 h in an argon atmosphere and quenched in ice-cold water.

* Corresponding author.
E-mail address: morozkin@general.chem.msu.ru (A.V. Morozkin).

0966-9795/$ – see front matter © 2010 Elsevier Ltd. All rights reserved.
doi:10.1016/j.intermet.2010.10.013

Table 1
Crystallographic and magnetic properties of La_3NiGe_2-type compounds.

	a, nm	*b*, nm	*c*, nm	R_F, %	Θ_P, K	M_{eff}/R, μ_B	T_{CN}, K	$-\Delta S_m$, J/kg•K	ΔT_{ad}, K	Magnetic structure	Refs.
Ce_3CoGe_2	1,1951	0,4302	1,1477		−59	2,62	$T_C = 6$ K $T_N = 3.4$ K				[4]
Pr_3CoGe_2	1,1942	0,4293	1,1418		18	3,63	$T_{CN} = 28$ K			$(\mathbf{F}_a-\mathbf{AF}_c)^{K0}$, $\mathbf{K}_0 = [0, 0, 0]$, $(M^F_{Pr})_a = 2.59(9)$ μ_B, $(M^{AF}_{Pr})_c = 1.58(4)$ μ_B, $\lvert M_{Pr}\rvert = 3.03(9)$ μ_B at 2 K	[4] This work
Nd_3CoGe_2	1,1856	0.427	1136		21	3,87	$T_{CN} = 35{,}5$ K			$(\mathbf{F}_a-\mathbf{AF}_c)^{K0}$, $\mathbf{K}_0 = [0, 0, 0]$, $(M^F_{Nd})_a = 2.6(1)$ μ_B, $(M^{AF}_{Nd})_c = 1.65(6)$ μ_B, $\lvert M_{Nd}\rvert = 3.1(1)$ μ_B at 2 K	[4] This work
Sm_3CoGe_2	1.1706(1)	0.42267(5)	1.1242(1)	3.9							This work
Gd_3CoGe_2[a-]	1,15845(5)	0,41905(2)	1,12088(5)	2.4			$T_{CN} = 150$ K	−4.9(5T)			This work
Tb_3CoGe_2[a-]	1,14942(4)	0,41705(2)	1,11030(4)	3.8			$T_{CN} = 110$ K				This work
Dy_3CoGe_2	1.1431(2)	0.41500(5)	1.1040(2)	2.1							This work
Ce_3NiGe_2	1,1924	0,4311	1,1624				$T_N = 6.2$ $T_C = 5.2$ K				[1, 5]
Gd_3NiGe_2	1,1473	0,41963	1,1328				$T_C = 193$ K	−13(7.5 T)			[1, 7]
Gd_3NiSi_2	1,1378	0,41494	1,1325				$T_C = 215$ K	−6.3(4.6 T)	5 (4.6 T)		[1, 3, 8]

[a-] The crystallographic data used with permission - © JCPDS - International Centre for Diffraction Data.

Table 2
Atomic positions in Pr_3CoGe_2 and Gd_3CoGe_2.a) Pr_3CoGe_2 at 35 K b) Gd_3CoGe_2 at 300 K.

Atom	Site	x/*a*	y/*b*	z/*c*	x/*a*	y/*b*	z/*c*
R1	4c	0.376(2)	1/4	0.440(2)	0.3784(8)	1/4	0.4399(8)
R2	4c	0.064(2)	1/4	0.364(2)	0.0522(8)	1/4	0.3730(8)
R3	4c	0.220(2)	1/4	0.707(2)	0.2207(8)	1/4	0.6972(9)
Co	4c	0.150(5)	1/4	0.127(5)	0.136(2)	1/4	0.126(2)
Ge1	4c	0.473(1)	1/4	0.679(1)	0.481(1)	1/4	0.689(2)
Ge2	4c	0.307(1)	1/4	0.010(2)	0.304(1)	1/4	−0.002(2)

The quality of the samples was evaluated using X-ray diffraction and electron microprobe analysis. The X-ray data were obtained on a DRON-3.0 diffractometer (Cu K_α radiation, $2\Theta = 5$–120 deg, step 0.02 deg, 10 s per step) and on a Guinier camera with silicon as standard ($a = 5.4308$ Å and Cu$K\alpha_1$ radiation). The unit cell data were derived using the Rietan-program [10] in the isotropic approximation (Tables 1 and 2). A «Camebax» microanalyser was employed to perform microprobe X-ray spectral analysis of the samples. The quantitative microprobe analysis of the samples gave 50 ± 1…2 at % of rare earth, 16 ± 1% at. of cobalt and 33 ± 1 at % of germanium.

The neutron powder diffraction studies of Pr_3CoGe_2 and Nd_3CoGe_2 were carried out from 35 to 40 K down to 2 K in a zero magnetic field at the Institute Laue-Langevin, Grenoble, France, using the high resolution powder diffractometer *D1B* [11], operating at a wavelength $\lambda = 0.2525$ nm ($2\theta = 4.6$–87 deg). The diffraction patterns were refined with the FULLPROF 98-program [12].

The dc magnetisation was measured on a commercial SQUID magnetometer (Quantum Design) in the temperature range of 5–300 K in the applied field up to 5 T.

3. Results and discussion

3.1. Crystal structure

The X-ray diffraction patterns of present R_3CoGe_2 showed that they adopt the La_3NiGe_2 (Gd_3NiSi_2)-type structure [3]. The refined unit cell data of R_3CoGe_2 are given in Table 1. The refined atomic positions of R_3CoGe_2 are close to those of Pr_3CoGe_2 and Gd_3CoGe_2 (Table 2). Interatomic distances in R_3CoGe_2 are summarized in Table 3 and they close to the sum of metallic radii [13].

The La_3NiGe_2-type R_3CoGe_2 structure (sp. group *Pnma*) consists of the rare-earth, cobalt and germanium substructures with the **mmm** ($\mathbf{D_{2h}}$) point group containing the following symmetry operators: $\{\mathbf{1}, \mathbf{2}_x, \mathbf{2}_Y, \mathbf{2}_Z, \overline{1}, \mathbf{m}_x, \mathbf{m}_Y, \mathbf{m}_Z\}$ [14]. The $\mathbf{D_{2h}}$ point group has seven invariant subgroup of index 2: $\mathbf{N}_1 = \{\mathbf{1}, \mathbf{2}_x, \mathbf{2}_Y, \mathbf{2}_Z\}$, $\mathbf{N}_2 = \{\mathbf{1}, \mathbf{m}_x, \mathbf{m}_Y, \mathbf{2}_Z\}$, $\mathbf{N}_3 = \{\mathbf{1}, \mathbf{m}_Y, \mathbf{m}_Z, \mathbf{2}_x\}$, $\mathbf{N}_4 = \{\mathbf{1}, \mathbf{m}_x, \mathbf{m}_Z, \mathbf{2}_Y\}$, $\mathbf{N}_5 = \{\mathbf{1}, \mathbf{m}_x, \mathbf{2}_x, \overline{1}\}$,

Table 3
Interatomic distances, D ± 5 × 10^{-4} nm, in the Gd_3CoGe_2, their ratio to sum of the metallic radii of the corresponding atoms $\Delta = D/(R_{atom1} + R_{atom2})$ and coordination numbers δ.

Atom	-Atom	D, nm	Δ	δ	Atom	-Atom	D, nm	Δ	δ	Atom	-Atom	D, nm	Δ	δ
Gd1-	2Co	0.2961	0,97		Gd2-	1Co	0.2934	0,96		Gd3-	2Co	0.2790	0,92	
	1Ge1	0.3022	1.00			2Ge1	0.2965	0,98			1Ge1	0.3017	1.00	
	1Ge1	0.3035	1,00			2Ge2	0.3021	1.00			1Ge1	0.3056	1,01	
	2Ge2	0.3046	1,01			1Ge2	0.3218	1,06			2Ge2	0.3075	1,02	
	1Co	0.3074	1,01			2Gd2	0.3736	1,04			1Gd1	0.3414	0,95	
	1Gd3	0.3414	0,95			1Gd1	0.3853	1,07			2Gd1	0.3621	1,01	
	2Gd3	0.3621	1,01			2Gd3	0.3873	1,08			1Ge2	0.3507	1,16	
	2Gd1	0.3761	1,05			2Gd3	0.3898	1,08			2Gd2	0.3873	1,08	
	1Gd2	0.3853	1,07			1Gd3	0.4125	1,15			2Gd2	0.3898	1,08	
	1Gd2	0.4044	1,12	14		1Gd1	0.4044	1,12	15		1Gd2	0.4125	1,15	15
Co–	1Ge2	0.2418	0,98		Ge1 -	2Co	0.2593	1,05		Ge2 -	1Co	0.2418	0,98	
	2Ge1	0.2593	1,05			1Gd2	0.2965	0,98			2Gd2	0.3021	1.00	
	2Gd3	0.2790	0,92			1Gd3	0.3017	1.00			2Gd1	0.3046	1,01	
	1Gd2	0.2934	0,96			2Gd1	0.3022	1.00			2Gd3	0.3075	1,02	
	1Gd1	0.2961	0,97			1Gd1	0.3035	1,00			1Gd2	0.3218	1,06	
	1Gd1	0.3074	1,01	8		1Gd3	0.3056	1,01	8		1Gd3	0.3507	1,16	9

Table 4
Atomic positions of the Rj atoms (j = 1, 2, 3) in the La_3NiGe_2-type R_3CoGe_2 unit cell (space group *Pnma*) with the corresponding symmetry operators.

Atom	X/*a*	Y/*b*	Z/*c*	Symmetry operation
Rj^1	X_{Rj}	1/4	Z_{Rj}	$Rj^1 = (\mathbf{1}/0)Rj^1 = (\mathbf{m}_Y/[0\ 1/2\ 0])Rj^1$
Rj^2	1/2 - X_{Rj}	3/4	1/2 + Z_{Rj}	$Rj^2 = (\mathbf{2}_Z/[1/2\ 0\ 1/2])Rj^1 = (\mathbf{m}_X/[1/2\ 1/2\ 1/2])Rj^1$
Rj^3	1/2 + X_{Rj}	1/4	1/2 − Z_{Rj}	$Rj^3 = (\mathbf{m}_Z/[1/2\ 0\ 1/2])Rj^1 = (\mathbf{2}_X/[1/2\ 1/2\ 1/2])Rj^1$
Rj^4	$-X_{Rj}$	3/4	$-Z_{Rj}$	$Rj^4 = (\bar{1}/0)Rj^1 = (\mathbf{2}_Y/[0\ 1/2\ 0])Rj^1$

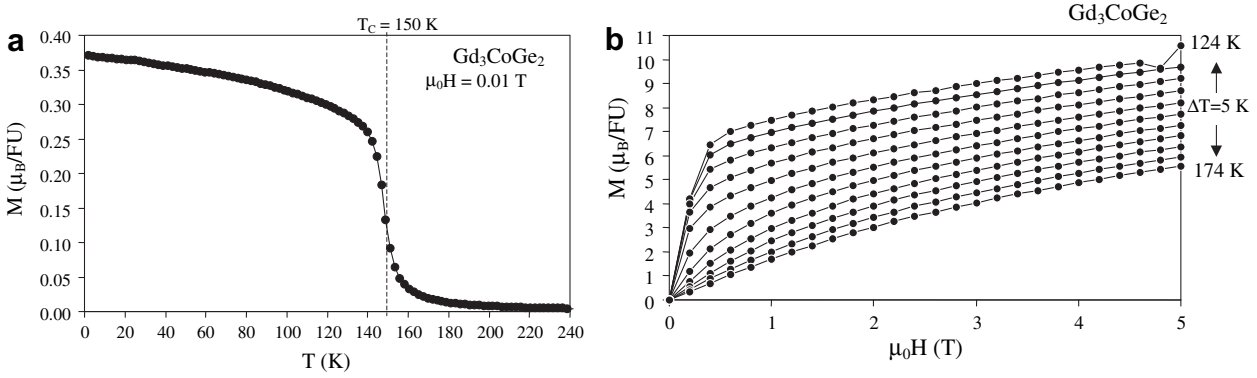

Fig. 1. (a) Magnetization vs. temperature and (b) vs. magnetic field around the magnetic transition for Gd_3CoGe_2.

$\mathbf{N}_6 = \{\mathbf{1}, \mathbf{m}_Y, \mathbf{2}_Y, \bar{1}\}$, $\mathbf{N}_7 = \{\mathbf{1}, \mathbf{m}_Z, \mathbf{2}_Z, \bar{1}\}$: $\{\mathbf{D_{2h}}\} = \{\mathbf{N}_1, \mathbf{m}_Z \times \mathbf{N}_1\} = \{\mathbf{N}_2, \mathbf{m}_Z \times \mathbf{N}_2\} = \{\mathbf{N}_3, \mathbf{m}_x \times \mathbf{N}_3\} = \{\mathbf{N}_4, \mathbf{m}_Y \times \mathbf{N}_4\} = \{\mathbf{N}_5, \mathbf{m}_Y \times \mathbf{N}_5\} = \{\mathbf{N}_6, \mathbf{m}_x \times \mathbf{N}_6\} = \{\mathbf{N}_7, \mathbf{m}_x \times \mathbf{N}_7\}$. The *Pnma* space group contains the following symmetry operations with fractional translations: $\mathbf{n} = (\mathbf{m}_x/[1/2\ 1/2\ 1/2])$, $\mathbf{m} = (\mathbf{m}_Y/[0\ 1/2\ 0])$, $\mathbf{a} = (\mathbf{m}_Z/[1/2\ 0\ 1/2])$, $\mathbf{2}_x^* = (\mathbf{2}_x/[1/2\ 1/2\ 1/2])$, $\mathbf{2}_Y^* = (\mathbf{2}_Y/[0\ 1/2\ 0])$ and $\mathbf{2}_Z^* = (\mathbf{2}_Z/[1/2\ 0\ 1/2])$ (Table 4).

3.2. Magnetization

According to the magnetization measurements, Gd_3CoGe_2 undergoes a ferromagnetic-type transition at 150 K (Fig. 1a) and Tb_3CoGe_2 at 110 K [15]. The saturation magnetisation values at 5 T (M = 9.7 μ_B/FU and $M \sim 3.2$ μ_B/Gd at 130 K) are indicative of the presence of an antiferromagnetic component in the magnetic structure of Gd_3CoGe_2 and, potentially, of other R_3CoGe_2 compounds. The magnetic transition temperatures in Ce_3CoGe_2, Pr_3CoGe_2 and Nd_3CoGe_2 do not follows the de Gennes rule (Fig. 2).

3.3. Magnetocaloric effect

The magnetocaloric effect, MCE, for Gd_3CoGe_2 was evaluated from the magnetization vs. field (M vs. H) data measured around the Curie temperature with 5 K increments. The magnetic field changed from 0 to 5 T in 0.2 T steps. MCE in terms of the isothermal entropy change, ΔS, can be calculated from the magnetization data through the Maxwell equation [16]: $(\frac{\partial S(T,H)}{\partial H})_T = (\frac{\partial M(T,H)}{\partial T})_H$. Integration of the partial derivative of magnetization, M, with respect to temperature, T, over a change in the magnetic field, H, yields the following expression for ΔS: $\Delta S(T)_{\Delta H} = \int_{H_1}^{H_2} (\frac{\partial M(T,H)}{\partial T})_{H,P} dH$. In practice a numerical integration is performed: $\Delta S(T)_{\Delta H} = \sum_i \frac{M_{i+1} - M_i}{T_{i+1} - T_i} \Delta H$, where ΔH is a change in magnetic field and M_i and M_{i+1} are the values of magnetization at temperatures T_i and T_{i+1}, respectively.

The magnetocaloric effect for Gd_3CoGe_2 in terms of the isothermal entropy change, -ΔS, (Fig. 3) reaches the maximum value of 4.9 J/kg·K in the 139–144 K temperature region (Fig. 3). The maximum |ΔS| value is lower than those observed for isostructural Gd_3NiGe_2 and Gd_3NiSi_2 [7,8] (Table 1).

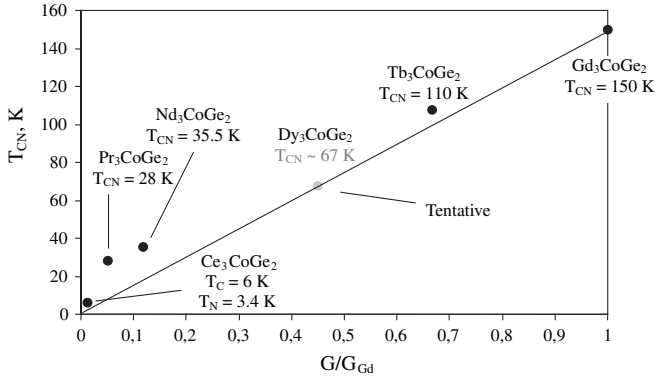

Fig. 2. Magnetic ordering temperatures of R_3CoGe_2 vs. de Gennes factor. The tentative magnetic ordering temperatures of Tb_3CoGe_2 and Dy_3CoGe_2 are derived from the de Gennes rule.

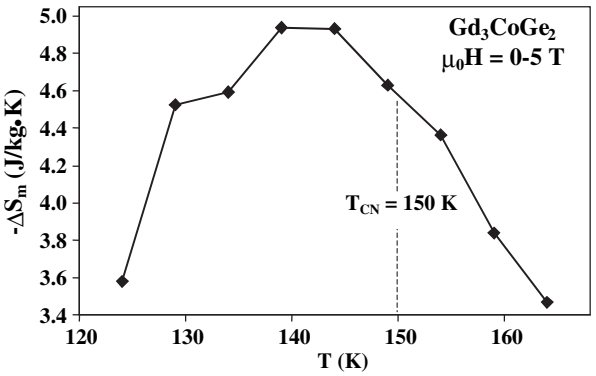

Fig. 3. Magnetocaloric effect of Gd_3CoGe_2 as a function of temperature.

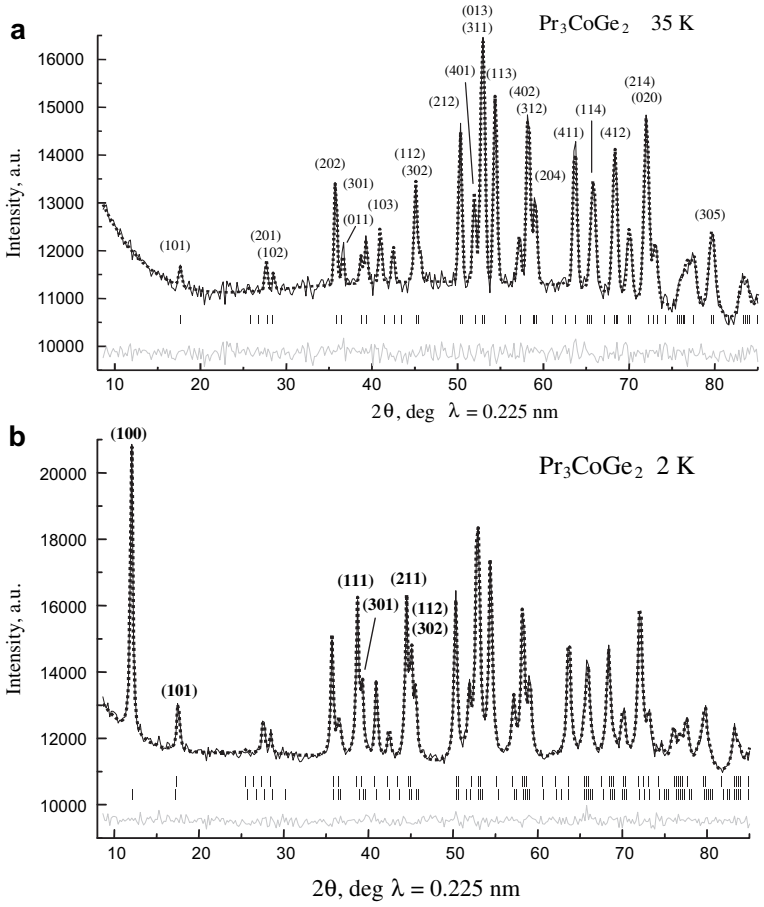

Fig. 4. Neutron diffraction patterns of Pr_3CoGe_2 at (a) 35 K (paramagnetic state) and (b) 2 K (commensurate ferrimagnetic). Strong magnetic reflections are recognized in Figure (b).

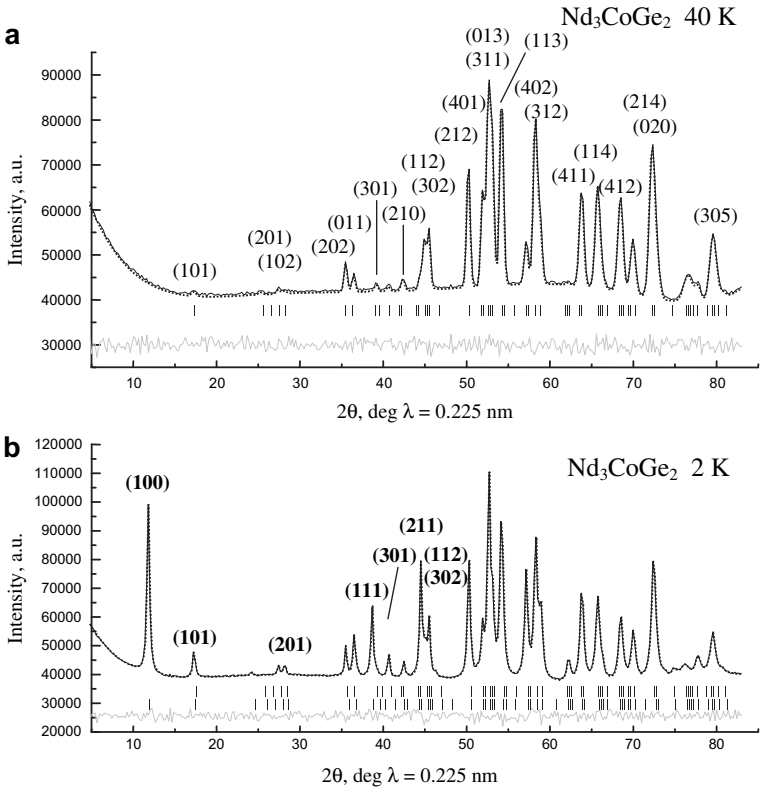

Fig. 5. Neutron diffraction patterns of Nd_3CoGe_2 at (a) 40 K (paramagnetic state) and (b) at 2 K (commensurate ferrimagnetic). Strong magnetic reflections are recognized in Figure (b).

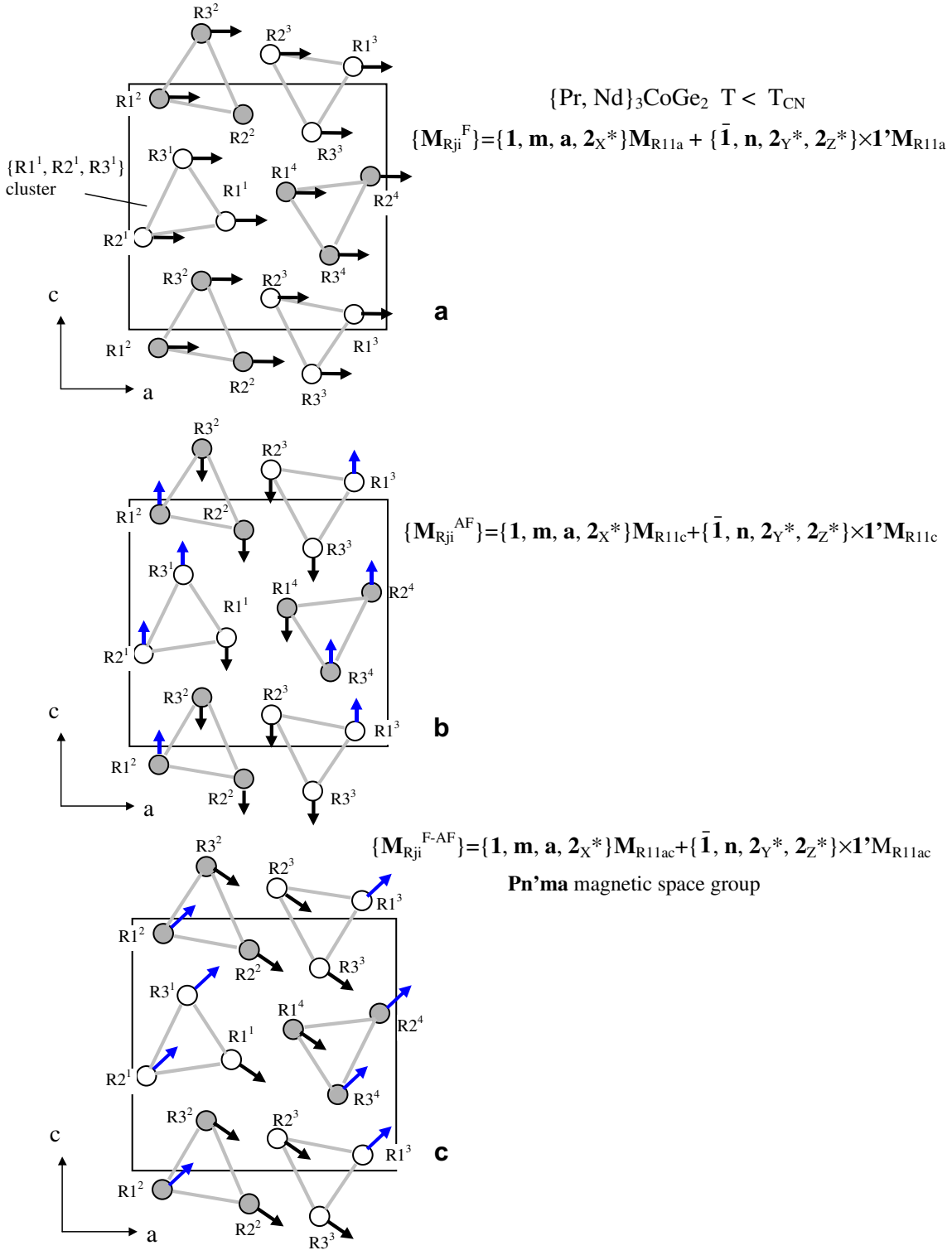

Fig. 6. Magnetic structure of Pr_3CoGe_2 and Nd_3CoGe_2 below T_{CN}: ferromagnetic part (a), antiferromagnetic part (b) and general (ferrimagnetic) Pn'ma magnetic space group ordering of rare-earth sublattice (c). The white R atoms have $Y_{Rji} = 1/4$, gray R atoms have $Y_{Rji} = 3/4$.

3.4. Magnetic structure

Figs. 4 and 5 show the neutron diffraction patterns of Pr_3CoGe_2 and Nd_3CoGe_2 recorded at different temperatures in zero magnetic field. Both compounds show commensurate magnetic ordering below $T_{CN} \sim 28$ K (Pr_3CoGe_2) and $T_{CN} \sim 35$ K (Nd_3CoGe_2).

Symmetry of the R1, R2 and R3 substructures in the R_3CoGe_2 is identical to the symmetry of $\{R1^i, R2^i, R3^i\}_{j\ =\ 1,\ 2,\ 3,\ 4}$ clusters (Fig. 6a). The cobalt substructure consists of isolated atoms (the shortest Co–Co distance, D_{Co-Co}, is the b parameter and $\Delta = D_{Co-Co}/(2R_{Co}) = 1.67$) and no magnetic ordering with the cobalt substructure is expected. Refinement of the neutron

Table 5
Crystallographic and magnetic parameters of the Pr_3CoGe_2 and Nd_3CoGe_2 phases: Lattice parameters *a, b, c* at different temperatures, antiferromagnetic ($\mathbf{M}_Z^{AF}$) and ferromagnetic ($\mathbf{M}_x^F$) components of the magnetic moment **M** for the Pr and Nd atoms. Reliability factors R_F (crystal structure) and R_F^m (magnetic structure) are given in percents (%).

State	T, K	Cell parameters	R_F, %	Atom	$\mathbf{M}_c^{AF}$, μ_B	$\mathbf{M}_a^F$, μ_B	|**M**|, μ_B	R_F^m, %
a) Pr_3CoGe_2								
Para	300[a-]	a = 1.1942(3) nm						
		b = 0.4293(2) nm						
		c = 1.1418(4) nm						
	35	a = 1.1909(4) nm	7.6					
		b = 0.4292(1) nm						
		c = 1.1343(4) nm						
F-AF	2	a = 1.1896(4) nm	3.9	$Pr1^1,1^4,2^2,2^3,3^2,3^3$	−1.58(4)	2.59(9)	3.03(9)	5.7
		b = 0.4283(1) nm		$Pr1^2,1^3,2^1,2^4,3^1,3^4$	1.58(4)	2.59(9)	3.03(9)	
		c = 1.1317(4) nm						
b) Nd_3CoGe_2								
Para	300[a-]	a = 1.1856(4) nm						
		b = 0.4270(1) nm						
		c = 1.1360(5) nm						
	40	a = 1.1823(5) nm	7.6					
		b = 0.4261(2) nm						
		c = 1.1321(5) nm						
F-AF	2	a = 1.1819(4) nm	3.9	$Nd1^1,1^4,2^2,2^3,3^2,3^3$	−1.65(6)	2.6(1)	3.1(1)	7.7
		b = 0.4254(1) nm		$Nd1^2,1^3,2^1,2^4,3^1,3^4$	1.65(6)	2.6(1)	3.1(1)	
		c = 1.1320(3) nm						

[a-] X-ray data.

diffraction patterns showed that both Pr_3CoGe_2 and Nd_3CoGe_2 have a ferromagnetic component along the *a* axis and an antiferromagnetic component along the *c* axis (Fig. 6a and b). Both components have the same magnetic point group. The unprimed point group coincides with the $\mathbf{N}_3$ invariant subgroup of index 2 whereas the primed subgroup is $\mathbf{m}_x \times \mathbf{N}_3$ (see the *Crystal structure* section above): $\mathbf{m'mm} = \{\mathbf{N}_3 + \mathbf{m}_x \times \mathbf{N}_3 \times \mathbf{1'}\} = \{\mathbf{1}, \mathbf{m}_Y, \mathbf{m}_Z, \mathbf{2}_x\} + \{\bar{1}, \mathbf{m}_x, \mathbf{2}_Y, \mathbf{2}_Z\} \times \mathbf{1'}$. So, Pr_3CoGe_2 and Nd_3CoGe_2 demonstrate the commensurate ferrimagnetic type *ac* ordering with the magnetic point group **m'mm** and the magnetic space group **Pn'ma** (Fig. 6c). Details on the magnetic structures are given in Table 5.

The refined magnetic moment are 3.03(9) μ_B/Pr^{3+} and 3.19 (1) μ_B/Nd^{3+} at 2 K, and they are close to the theoretical magnetic moments of the Pr^{3+} and Nd^{3+} ions: $M_{Pr} = gJ = 3.20\ \mu_B$ (Pr) and $M_{Nd} = gJ = 3.27\ \mu_B$ (Nd) [9].

4. Conclusions

The ferrimagnetic nature of novel La_3NiGe_2-type R_3CoGe_2 is evident both from the magnetic and neutron diffraction studies. Pr_3CoGe_2 and Nd_3CoGe_2 exhibit a commensurate ferrimagnetic ordering in the *ac* plane (**Pn'ma** magnetic space group). According to the de Gennes rule, the magnetic structures of $\{Gd, Tb, Dy\}_3CoGe_2$ should differ from those of $\{Pr,Nd\}_3CoGe_2$. The magnetocaloric effect of Gd_3CoGe_2 is smaller than that of isostructural Gd_3NiGe_2 and Gd_3NiSi_2.

Acknowledgements

This work was supported by the *Russian Fund for Basic Research* through the project N° 09-03-00173-a. This work supported by a ICDD grant N 05-07. The crystallographic data of Gd_3CoGe_2 and Tb_3CoGe_2 were used with permission - © JCPDS - International Centre for Diffraction Data.

References

[1] Pearson's Handbook of crystallographic data for intermetallic phases. Metals Park, Oh 44073: American Society for Metals; 1985. 1–3.
[2] Gladyshevsky EI, Bodak OI. Kristallohimia intermetallicheskih soedinenii redkozemel'nyh metallov. LSU: L'viv; 1982 [in Russian]8–29.
[3] Klepp K, Parthe E. Acta Crystallogr, B 1981;37:1500.
[4] Dhar SK, Paulose PL, Palenzona A, Manfrinetti P, Cimberle R. J Magn Magn Mat 2004;270:43–50.
[5] Pikul AP, Kaczorowski D, Rogl P. Physica B 2002;312-313:422.
[6] David Lide R, editor. Hanbook of chemistry and physics. 75th ed. Boca Raton, Florida, USA: CRC Press, Inc.; 1994.
[7] Gschneidner KA, Pecharsky VK, Gailloux MJ, Takeya H. Utilization of the magnetic entropy in active magnetic refrigerator materials. Adv. Cryog. Eng.; 1995.
[8] Tencé S, Gorsse S, Gaudin E, Chevalier B. Intermetallics 2008;17(3):115–9.
[9] Legvold S. Rare earth metals and alloys. In: Wohlfarth P, editor. Ferromagnetic materials. Amsterdam: North-Holland Publ. Co.; 1980. p. 183–295.
[10] Izumi F. In: Young RA, editor. The Rietveld method. Oxford: Oxford University Press; 1993. p. 13.
[11] www.ill.fr, Yellow Book.
[12] Rodriguez-Carvajal J. Physica B 1993;192:55–69.
[13] Emsley J. The elements. 2nd ed. Oxford: Clarendon Press; 1991.
[14] Kireev PS. Introduction of theory group and it's application in solid state physic. Moscow: High Scool; 1979 [In Russian].
[15] Mozharivskyj Yu, Svitlyk V. [Unpublished data].
[16] Tishin AM, Spichkin YL. The magnetocaloric effect and its applications. Bristol and Philadelphia: Institute of Physics Publishing; 2003. 480.